Review

High-resolution imaging of entire organs by 3-dimensional imaging of solvent cleared organs (3DISCO)

Ali Ertürk [a,*], Frank Bradke [b,*]

[a] Department of Neurobiology, Genentech, Inc., 1 DNA Way, South San Francisco, CA 94080, USA
[b] Deutsches Zentrum für neurodegenerative Erkrankungen (DZNE), Axonal Growth and Regeneration, Ludwig-Erhard-Allee 2, 53175 Bonn, Germany

ARTICLE INFO

ABSTRACT

One goal in neuroscience is to dissect neuronal connections within the nervous system in health and disease. To accomplish this, neurons and their extensions need to be imaged and followed in the entire brain and spinal cord. While non-invasive imaging methods such as MRI do not have sufficient resolution to trace individual cells, standard histology – serial tissue sectioning and tracing in consecutive sections – is time consuming and prone to mistakes. Here, we review an alternative method called "3D imaging of solvent cleared organs" or "3DISCO" that can achieve high-resolution imaging of neuronal connections in several millimeters of depth without tissue sectioning. 3DISCO is fast: imaging of an entire organ at a cellular resolution can be completed within a few hours. 3DISCO is versatile: it is applicable to various tissues including the spinal cord, brain, lung, mammary glands, immune organs and tumors; it can be executed using various microscopy techniques, including light-sheet, widefield epifluorescence, confocal, 2-photon, light microscopy and optical coherent tomography. Here, we review the application of 3DISCO along with other popular clearing and imaging methods, their limitations and the obstacles that remain.

© 2012 Elsevier Inc. All rights reserved.

Contents

Introduction

Tracing neuronal projections are closely linked with the evolution of neuroscience. Ramon y Cajal, the pioneering neuroanatomist shed the first insights into the complex organization of the nervous tissue (Sotelo, 2003). He labeled and observed neuronal cell types and tissues at microscopic scale. Over the decades after Cajal's work, numerous researchers have characterized an increasing amount of anatomical details of the neurons and synapses at the micrometer scale. Even though this knowledge gives a good understanding of how individual neurons and groups of neurons in a small compartment of the brain, e.g. hippocampus, and spinal cord work, we still lack a complete map of the entire nervous system, and therefore we are limited in understanding its functions. This shortcoming is mainly due to lack of tools to image long neuronal projections, which can span the entire brain and spinal cord over several centimeters in rodents and over meters

* Corresponding authors.
  E-mail addresses: Erturk.Ali@gene.com (A. Ertürk), Frank.Bradke@dzne.de
(F. Bradke).

in mammalians. As a result, our understanding of cognitive and behavioral functions of the nervous system, which works as an entire unit, has been incomplete. Similarly, it has been a challenge to develop therapies to traumatic or chronic diseases of the nervous system, because we do not know how a healthy nervous system is wired. For example, developing successful therapeutic interventions for spinal cord injury (SCI) requires restoring disrupted sensory and motor axons, which connect the peripheral organs of the body to the brain and vice versa. To achieve this, in experimental models at first, it is necessary to map entire spinal cord connections at micron or even sub-micron resolution over centimeters, which is a challenging task. In the last decades, two imaging methods have been popular for imaging large tissues and organs: First, the non-invasive imaging methods, including magnetic resonance imaging (MRI), computer tomography (CT) and positron emission tomography (PET), which can image organs as large as the entire brain and spinal cord. These techniques have a unique advantage of being applied repeatedly on the same organism, which helps to determine the changes over time. However, these methods have a limited resolution (~75 μm), which is not even sufficient to identify individual cell bodies (Tyszka et al., 2005). In a second approach to map large organs, researchers aim to use high-resolution scanning techniques, such as confocal microscopy and electron microscopy (EM), in combination with serial tissue sections and subsequent reconstruction of the entire organ by combining overlapping scans. This method provides high-resolution images (at submicron scale) but it is extremely laborious and prone to mistakes during mechanical tissue sectioning and stitching of the data (Briggman and Denk, 2006). For example, it has been estimated on the basis of the state of the art technology that the reconstruction of the entire anatomical connections of a rodent brain or spinal cord (~1 cm^3) would take 1000 years with an electron microscope at a resolution of $15 \times 15 \times 50$ nm^3 and about 3 years with a confocal microscope at resolution of $250 \times 250 \times 500$ nm^3 (Silvestri et al., 2012). Therefore, studies aiming to induce axon regeneration after SCI could only assess morphology of axons over alternating tissue sections, such as collecting only a few sections (~20–50 μm thickness) of ~1500 μm thick mouse spinal cord (Fig. 1). When a spinal cord is sectioned to assess the regeneration of axons, spared axonal fragments can be misjudged as regenerating axons due to lack of a complete 3D visualization (Tuszynski and Steward, 2012). Moreover, other crucial information, including the length and trajectories of regenerating axons, will be extremely difficult to assess on tissue sections (Fig. 1).

In this review, we will focus on an alternative approach, 3-dimensional imaging of solvent cleared organs (3DISCO). 3DISCO is a recently evolving technique that is based on optical clearing and subsequent imaging of unsectioned transparent organs. It achieves micrometer resolution scans of histologically unsectioned tissues as large as rodent spinal cord and brain.

3DISCO overview

The main limitation of various optical imaging techniques is the difficulty of imaging thick tissues with high-resolution. Tissue clearing, whose first applications date back to almost a century, has become a prominent solution to light scattering (Spalteholz, 1914). It aims to match the refractory indexes of different tissue layers by making biological tissue transparent. In general, tissue clearing methods are based on two steps: tissue dehydration/delipidation, and impregnation by optical immersion. This is achieved by a series of chemical treatments, such as ethanol or tetrahydrofuran for dehydration and benzyl alcohol + benzyl benzoate mixture (BABB) or dibenzyl ether (DBE) for optical immersion. After rendering large biological samples transparent by tissue clearing, optical imaging deep within the tissue becomes possible. Two imaging methods, light-sheet ultramicroscopy, and 2-photon microscopy, have been efficient at imaging large cleared tissues with high-resolution in a short time. The details of optical clearing and imaging of transparent organs are discussed below.

Experimental procedure

Pre-3DISCO, step 1: tissue labeling

3D imaging of transparent organs can be exploited on embryonic or adult tissues from different model organisms, including rodents, flies and fish (Erturk et al., 2012; Gonzalez-Bellido and Wardill, 2012; Jahrling et al., 2010). The first step to obtain high-resolution 3DISCO scans is to label the organ of interest with a fluorophore (Table 1). 3DISCO is compatible with various labeling methods, including transgenic models expressing the fluorescent protein in the tissue of interest, deep tissue antibody labeling or synthetic dye tracing. For 3DISCO, the tissue should have a strong fluorescent labeling, which could be easily detected. Specimens that are successfully cleared and imaged in 3D include mice expressing GFP in a subset of neurons (Dodt et al., 2007; Erturk et al., 2012; Silvestri et al., 2012), *Drosophila* expressing GFP in muscles (Muller et al., 2010; Schonbauer et al., 2011) and dragonflies, squid and cuttlefish labeled with dye filling (Gonzalez-Bellido and Wardill, 2012). Alternatively, antibody staining can be used to label the tissue of interest even though it requires several days to weeks of staining and may not be achieved with every antibody. While regular antibody staining is restricted to the 20–30 μm surface of the tissue, there are dedicated protocols to increase penetration of the antibody
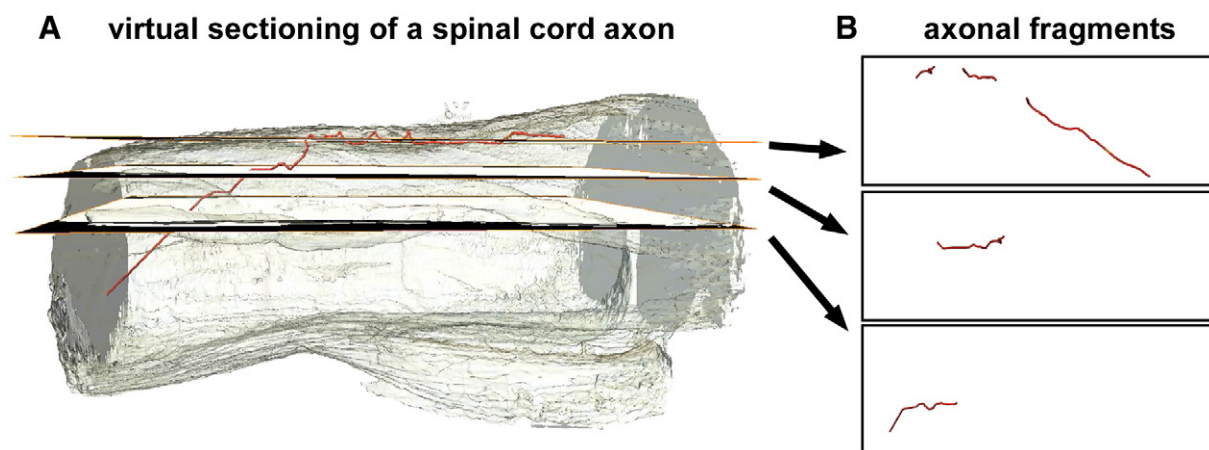
Fig. 1. Virtual tissue sectioning demonstrating possible obstacles. In a typical spinal cord injury study, the injured axons are labeled and subsequently the spinal cord tissue is fixed and sectioned to visualize the labeled axons (A). However, upon sectioning, the labeled axons are segregated onto different sections (B). It is very common that only few of those sections are evaluated to assess the regeneration and degeneration of the axons. Therefore, complete information regarding the length and trajectory of the axons (e.g. the red axon in A) could not be obtained. In addition, many of the observed axons could also be spared axons, which is a major problem and almost impossible to solve by just looking at the short axonal fragments in (B).

into deeper tissue layers (Dent et al., 1989; Sillitoe and Hawkes, 2002; Yokomizo et al., 2012). Interestingly, clearing of the tissues can be informative even without tissue labeling. Smith et al., used tissue clearing on rabbit heart to investigate the border zone between perfused and non-perfused tissue after a blockage of a coronary artery (Smith et al., 2012). They increased imaging resolution from ~100 μm to ~15 μm which uncovered complex 3D structure finger-like projections from non-perfused tissue penetrating into perfused regions.

Pre-3DISCO, step 2: tissue preparation

3DISCO is best applied on fixed organs, because the optical clearing agents are toxic to live tissue. Therefore, before clearing, the organ of interest should be fixed and dissected out as soon as the animal is killed at the end point of the experiment. The fixation (e.g. with paraformaldehyde (PFA)), a commonly used method to preserve the tissue, is also suitable but not required for tissues to be imaged with 3DISCO. Even though PFA perfusion helps to wash out blood or other intracellular fluids that usually reduce the clearing efficiency, it may also decrease the strength of the fluorescence and cause minor tissue deformation (Ott, 2008). Alternatively, the organs can simply be perfused with PBS solution alone or PBS solution containing heparin before PFA fixation if an organ with high blood circulation (e.g. brain or spleen) is studied.

3DISCO, step 1: tissue clearing

The limitation of imaging thick tissues with high-resolution is mainly due to strong light scattering through the thick tissues that contain various layers of cellular and extracellular structures with different refractive indexes. For example, live imaging of the spinal cord with the state of the art imaging techniques – such as 2-photon microscopy – is very informative but restricted to superficial axons due to scattering of imaging laser light throughout differently myelinated spinal cord layers (Erturk et al., 2007; Laskowski and Bradke, 2012; Ylera et al., 2009). The nucleus and cytoplasmic organelles have refractive indexes in a range of 1.38–1.41 at 589 nm wavelength. The refractive index of interstitial fluid is lower (1.33–1.35 at 589 nm wavelength) and the refractive index of key scattering agents, including protein fibrils and lipid membrane, is higher (1.39–1.47 at 589 nm wavelength) (Genina et al., 2010). Therefore, the imaging light travelling through thick tissue scatters and loses its excitation and emission efficiency. It results in a lower contrast and spatial resolution, as well as a shallower imaging depth (Boas, 1997; Tuchin, 2007). Water has a low refractive index (1.33) compared to cellular structures with proteins and lipids, hence, tissue dehydration is usually the first step to match the refractive indexes throughout the tissue (Genina et al., 2010). In the subsequent optical immersion step, the tissue is impregnated with an optical clearing agent (OCA), such as glucose (Zhao et al., 2011), glycerol (Bucher et al., 2000), 2,2′-thiodiethanol (TDE) (Gonzalez-Bellido and Wardill, 2012), BABB (Murray's clear) (Dodt et al., 2007; Erturk et al., 2012; Genina et al., 2010; Gerger et al., 2005) or DBE (Becker et al., 2012), which have approximately the same refractive index as the impregnated tissue containing proteins and lipids. Among those, BABB is the most frequently used for deep tissue imaging, because of the ability to increase the imaging depth substantially (up to 35 fold) compared to glycerol or glucose (up to 3–4 folds) (Genina et al., 2010).

Recently, Dodt et al. developed a clearing method based on usage of ethanol prior to BABB impregnation, which helped to image embryonic brains and excised hippocampi from mice expressing GFP in a subset of neurons with a resolution allowing imaging of individual spines (Dodt et al., 2007). However, this clearing protocol was not successful on heavily myelinated adult CNS tissue, and therefore could not be used on adult neuronal structures in health and disease. Therefore, we screened for new tissue clearing reagents and protocols and found that, among many OCAs tested, only tetrahydrofuran (THF) usage prior

to BABB substantially preserved the GFP signal and rendered the rodent adult spinal cord fully transparent (Erturk et al., 2012).

THF is a cyclic ether that readily dissolves lipids (Diaz et al., 1992; Starr and Hixon, 1943). It is relatively inert and lacks alcohol, aldehyde, and ketone groups. Its inertness helps to conserve the GFP signal, which is degraded by other lipid dissolving agents. This newly developed THF-based clearing method is quick, e.g. 3 h for the spinal cord, and can be combined with various labeling and microscopy techniques. Importantly, the THF based clearing protocol works with various tissues, including lymph nodes, lung tumors, and mammary glands.

A recent significant improvement on THF and BABB based clearing protocols has been the usage of DBE instead of BABB (Becker et al., 2012). The authors demonstrate that DBE is a better OCA than BABB because: 1) DBE preserves the fluorescent signal more, 2) it clears the tissues faster, 3) it provides better transparency when large tissues such as the brain are cleared, and 4) it is less toxic than BABB. Hence, DBE instead of BABB is preferable, especially when a tissue as large as mouse brain is cleared.

In a typical clearing protocol the tissue is first incubated with THF for dehydration. Subsequently, the dehydrated tissue is impregnated with BABB or DBE. We used the following basic protocol successfully on various tissues, including spinal cord and lymph nodes: Incubation of the tissue in 1) 50% THF for 30 min, 2) 80% THF for 30 min, 3) 3 times 100% THF for 30 min each and 4) BABB until the tissue becomes completely transparent, which usually takes 15–25 min (Erturk et al., 2012). Overall this protocol only takes ~3 h. The THF solutions are prepared in water by stirring or shaking for a few minutes. Similarly, to prepare BABB solution, one volume of benzyl alcohol (e.g. 50 ml) is mixed with two volumes of benzyl benzoate (e.g. 100 ml) by stirring or shaking for a few minutes (Erturk et al., 2012). It is also important to mention that organic solvents, including THF and BABB, are toxic chemicals and they should be handled with proper gloves (Nitrile 8 mil) in a properly ventilated fume-hood. In addition, they should be prepared and stored only in glassware.

In addition to clearing methods based on lipophilic organic solvents, e.g. BABB or DBE, recently, a water-mixable clearing technique based on urea named "Sca/e" has been developed (Hama et al., 2011). Even though this method could achieve a complete clearing and preservation of fluorescent signals in embryos (Hama et al., 2011), it failed to clear adult tissues even after several weeks to months of incubation (Becker et al., 2012). Nevertheless, as urea is a less toxic chemical compared to organic solvents, Sca/e can be a good alternative for studies aiming to image embryonic tissues. Note that all the clearing chemicals mentioned above are commercially available (e.g. from Sigma Aldrich) and are relatively inexpensive, hence one can easily test different protocols.

3DISCO, step 2: imaging of cleared tissues

Light-sheet microscopy, an imaging technique whose principle was developed over a century ago (Siedentopf and Zsigmondy, 1902), has gained popularity recently because it allows optical sectioning on large tissues. Over the last decades, different versions of light-sheet microscopy have emerged, including orthogonal-plane fluorescence optical sectioning (OPFOS) (Voie et al., 1993), selective plane illumination microscopy (SPIM) (Huisken et al., 2004), thin-light-sheet microscopy (TLSM) (Fuchs et al., 2002), confocal light sheet microscopy (CLSM) (Silvestri et al., 2012) and ultramicroscopy (Dodt et al., 2007; Mertz and Kim, 2010). In particular, ultramicroscopy has been effectively used to image various cleared CNS tissues, including embryonic brain, excised hippocampus and adult spinal cord at a resolution that allows the identification of individual neurons as well as their dendrites and axons (Dodt et al., 2007; Erturk et al., 2012). The basic idea behind light-sheet ultramicroscopy is to illuminate the sample from the side with a thin layer of light, which is typically obtained by a laser and a cylindrical lens (Fig. 2). Because the light travels only in the XY plane as thin as the defined z-step, only the imaging plane in focus is illuminated
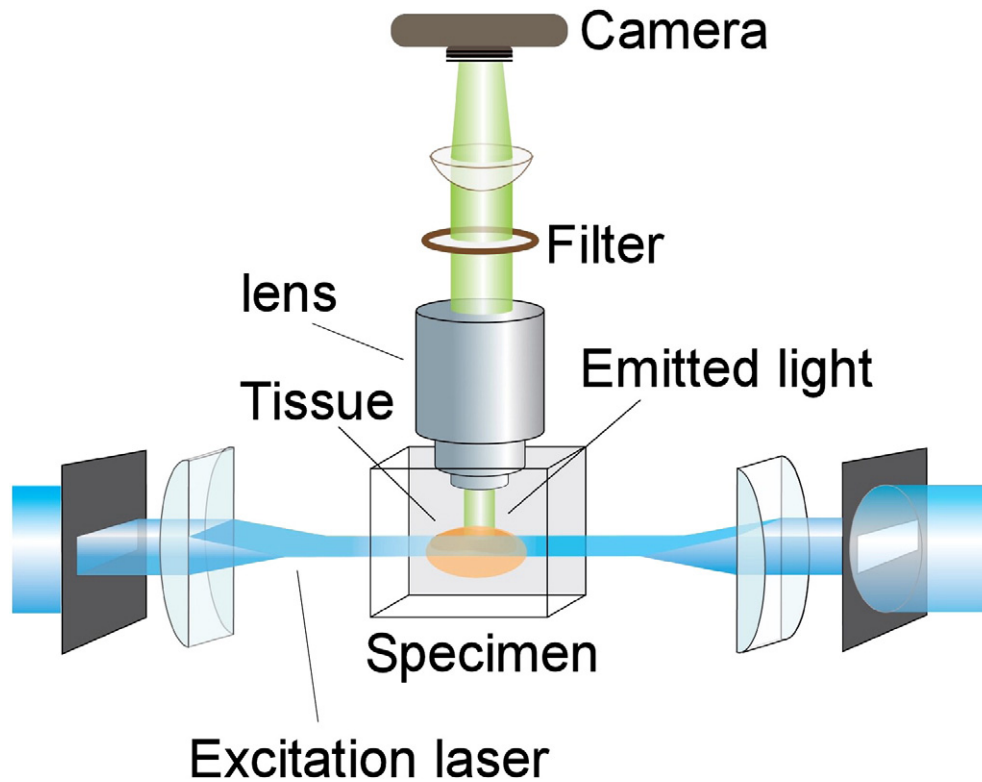
Fig. 2. Principles of ultramicroscopy. A drawing of the ultramicroscopy setup depicts the tissue positioning and light (Dodt et al., 2007; Erturk et al., 2012). The tissue is placed in the imaging chamber, which is filled with the final clearing solution (BABB or DBE). The excitation (imaging) laser coming from the side first passes through the glass walls of the imaging chamber and then throughout the cleared tissue without scattering. Finally, the emitted fluorescent signal is collected from above with a very sensitive camera.

(Fig. 2). Therefore, light-sheet ultramicroscopy imaging avoids scattering and bleaching by an out-of-focus signal and preserves intensity of the excitation laser, which would be absorbed by out-of-focus tissue. This illumination method results in high contrast imaging, thereby increasing the resolution obtained by low magnification objectives (1×, 2.5× or 5X) with a large imaging field (up to about 1 cm^2) and a low numerical aperture (NA) (Leischner et al., 2009). To compensate for the gradient decrease in imaging laser power, especially when tissues as large as adult mouse brain are imaged, the object is ideally illuminated from two opposing sides with overlapping lasers (Fig. 2), (Dodt et al., 2007; Menzel, 2011). During ultramicroscopy imaging, the cleared tissue is placed in a chamber filled with the clearing solution (e.g. BABB or DBE). The optical sectioning of the cleared tissue is then achieved by moving the chamber with tissue in the vertical space with the defined z-increments (Fig. 2). Using ultramicroscopy we imaged large (~5 mm) unlesioned and lesioned cleared spinal cord segments (Fig. 3, Videos 1 and 2) to follow the regenerating axons and glia reactions (Erturk et al., 2012). This allowed us to overcome the problems of tissue sectioning, which only shows fragments of axons (Fig. 1B). In addition, we could successfully image even larger tissues, including the entire adult mouse brain (Fig. 4, Video 3).

Cleared tissues have also been successfully imaged by conventional confocal and 2-photon microscopy (Erturk et al., 2012; Genina et al., 2010). In particular, 2-photon microscopy benefits from a significant increase in resolution and imaging depth upon tissue clearing even though the imaging field is small compared to ultramicroscopy (Video 4). Recently developed high NA objectives such as 20× with 1.0 NA can provide a z-resolution of 0.5 μm on cleared tissues but the imaging field is restricted to ~0.6 mm. For ultramicroscopy by contrast, the imaging field can be as large as ~15 mm (Video 3). Some examples of cleared tissues imaged by 2-photon microscopy are brain, brainstem, spinal cord

(Figs. 3C and D, Video 4), small intestine, large intestine, kidney, lung, mammary gland, testicle and ex vivo human skin (Cicchi et al., 2005; Erturk et al., 2012; Parra et al., 2010). Because 2-photon microscopy systems are commonly used and available in many research institutes, imaging of cleared tissues with a 2-photon system is a convenient solution compared to ultramicroscopy, which has only recently been made commercially available by Lavision Biotech. For 2-photon imaging, cleared tissue is mounted on a glass-slide with the final clearing solution (BABB or DBE) (Erturk et al., 2012). Silvestri et al. developed a new light-sheet imaging technique based on confocal microscopy (CLSM), which helps to eliminate the out-of-focus background signal. Combining CLSM with BABB tissue clearing, the authors imaged unsectioned cerebellum and brain from adult mice (Silvestri et al., 2012).

Moreover, tissue clearing improves resolution with optical coherence tomography (OCT) (Knuttel et al., 2004; Smith et al., 2012) and second harmonic generation (SHG) microscopy (Plotnikov et al., 2006; Yasui et al., 2004). The OCT is similar to ultrasound imaging, except that it uses near-infrared light (e.g. 1310 nm) instead of sound (Fujimoto et al., 2000; Regar et al., 2003). It is applicable to live tissue and is widely used in ophthalmology to enhance visualization of the various retinal layers (Bijlsma and Stilma, 2005). Clearing the tissue – as Smith et al. (2012) did on cardiac tissue – allows OCT scan to reach even deeper into the tissue due to a reduction of near-infrared light scattering (Wen et al., 2012). SHG, which uses an intense short-pulse laser light such as a femtosecond laser, obtains its imaging contrast from variations in biological structures' ability to generate second-harmonic light from the incident light (Campagnola and Loew, 2003). The anisotropic biological structures – such as collagen and muscle myosin – with large hyperpolarizability features can produce high imaging contrast with second-harmonic light, therefore, they are commonly imaged by SHG microscopy (Zipfel et al., 2003). In recent studies, authors injected glycerol
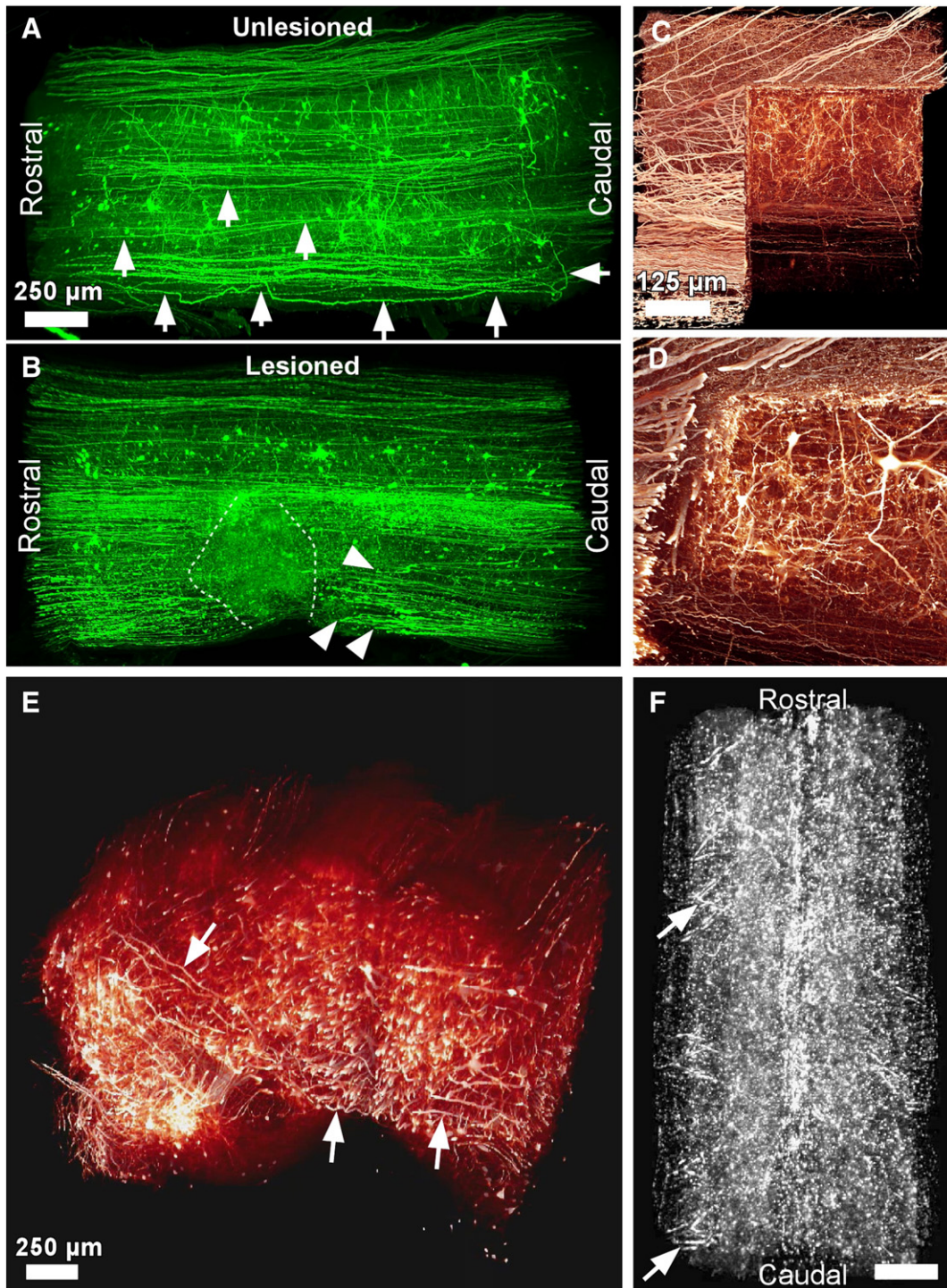
Fig. 3. 3DISCO samples acquired by ultra- and 2-photon microscopy. (A–B) 3–4 mm long unlesioned (A) and lesioned (B) adult spinal cord segments from GFP-M mice were cleared and imaged with ultramicroscopy. The arrows in (A) mark some of the axons over several millimeters; the lesion area and some of the retracting axons in (B) are marked by dashed lines and arrowheads, respectively. (C) is the visualization of the spinal cord with a corner-cut view from the top and (D) is from the side demonstrating the details of the neurons throughout the entire depth of the spinal cord acquired by 2-photon microscopy. (E, F) 3D reconstructions of a cleared brainstem (GFP-M mouse) (E) and a spinal cord (GFAP-GFP mouse) (F) scanned by ultramicroscopy. The arrows in (E) and (F) mark some of the individual axons and the blood vessels, respectively.

into various tissues, including rat skin, skeletal or cardiac muscle tissue and achieved a 2.5 fold increase in SHG imaging depth (Plotnikov et al., 2006; Yasui et al., 2004).

Post-3DISCO: data analysis

Because high-resolution imaging of large tissues results in very large data files (several gigabytes to terabytes), data analysis is both time consuming and overall not an easy task. Such large images need high-computing power and memory, which can be expensive. For example, usage of light-sheet microscopy to image cleared tissues (size of ~5 mm³) will result in 2–5 GB data. Such data can be analyzed with a powerful desktop workstation. We used Amira software to perform 3D visualization and tracing of the regenerating axons in the spinal cord (Erturk et al., 2012). However, when high-resolution confocal or 2-photon imaging of the small regions is used to subsequently stitch
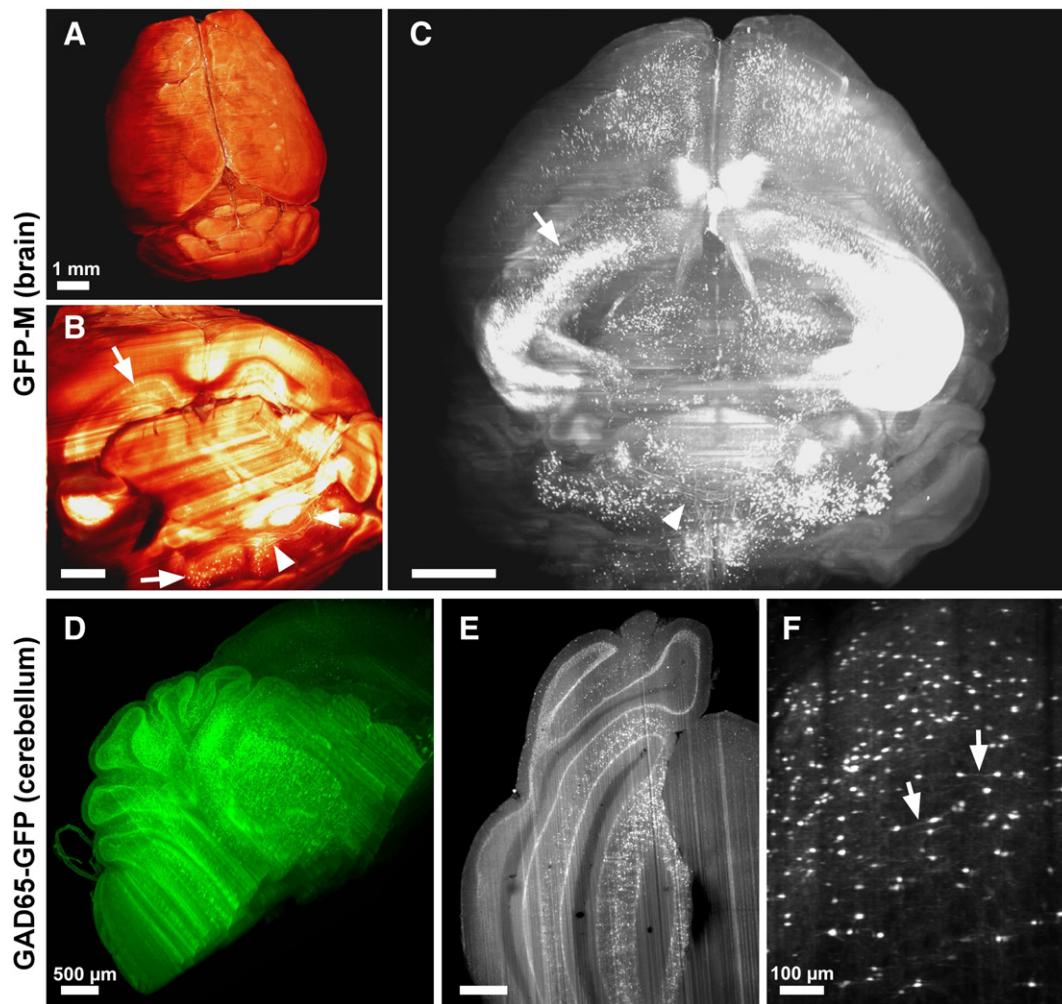
Fig. 4. 3DISCO of neurons in the brain. (A–C) The entire cleared brains from GFP-M mice were imaged using ultramicroscopy. 3D surface volume rendering of the entire brain is shown in (A) and with a corner-cut view in (B). The 3D morphology of inner brain structures (e.g. hippocampus) as well as the individual neuronal cell bodies (arrows in B) and some of the axonal extensions are evident (arrowheads in B). (C) The transparent 3D reconstruction of the brain showing the individual neurons (arrow) and neuronal extensions (arrowheads). (D–F) The 3DISCO samples from GAD65-GFP mice, which was cleared and imaged using ultramicroscopy. (D) is the transparent 3D reconstruction of the cerebellum, (E) is a 2D projection from the 3D scan of cerebellum and (F) is a high magnification view showing the individual inhibitory GAD65 positive neurons.

the overlapping images, the data can reach a terabyte for a mouse brain (Silvestri et al., 2012). In fact, the authors developed a custom tool to stitch the terabyte size data (Silvestri et al., 2012). There are also commercially available solutions to circumvent the problems of large data management, segmentation, 3D reconstruction and quantifications (Helmstaedter and Mitra, 2012). In addition, there are free software that enable most functions necessary for 3D analysis. For example, in their protocol for labeling and imaging of neurons in thick invertebrate tissue samples, Gonzalez-Bellida and Wardill used the previously developed, freely available software Vaa3D/V3D (Peng et al., 2010) to visualize, stitch and trace the neurons.

Limitations of 3DISCO

Tissue clearing and subsequent 3D imaging of large tissues have begun to provide extensive anatomical information about various tissues. In addition to recent improvements in clearing and imaging technologies, its overall application is of very low cost, quick, and suitable to various tissues. However, there are various limitations of 3DISCO, and some of them are awaiting improvements. First of all, the tissue clearing could most successfully be applied to fixed tissues, precluding analysis of tissues *in the living animal*. Nevertheless, there have been attempts to clear tissues in vivo, particularly using OCAs, which are considered as "nontoxic" such as glucose and glycerol. Authors have achieved a

1.7 fold resolution increase in reflection spectroscopy when they applied 40% glucose to eye sclera of rabbits in vivo (Genina et al., 2006). However, glucose application to live tissue usually causes irreversible tissue damage due to high osmotic stress (Genina et al., 2010). Similarly, usage of 75% glycerol improves resolution of non-invasive imaging techniques but induces toxic side effects (Galanzha et al., 2003; Vargas et al., 2002). Therefore, development of better bio-compatible clearing protocols, which are not toxic to live tissue can improve resolution of live imaging. Another important caveat in tissue clearing is shrinkage of the tissue (Vargas et al., 1999). Tissue swelling is a rare event but can also be observed with certain OCAs, especially glycerol (Wen et al., 2010) and urea (Hama et al., 2011). Even though change in tissue size after clearing can be calculated and corrected for, the shrinkage may not be even throughout the different tissue layers, and therefore, may not reflect real size-ratios in vivo. Another limitation of tissue clearing is that it is incompatible with electronmicroscopy (EM). The main reason for this incompatibility lies in the nature of the clearing procedure, which is based on dehydration and lipid extraction of the tissue.

Not every tissue can be cleared and imaged by 3DISCO efficiently. For example, clearing and imaging the organs with high red blood cell content such as spleen is difficult. Even after perfusion, the erythrocytes may retain in the tissue, which decreases the transparency of the cleared tissue, and thereby blocks the penetration of imaging light into deeper tissue layers. A related problem can arise when pathological tissue,

Table 1

Diagram depicting the experimental steps of 3DISCO.

The red zone represents the steps before the application of 3DISCO, which includes tissue labeling and preparation. 3DISCO (yellow zone) is applied when the labeled tissue is fixed and dissected or exposed on live organisms e.g. skin. After clearing, a proper imaging technique is used to visualize the cleared tissue, which is now optically accessible for deep tissue imaging. Finally, collected datasets are analyzed using free or commercially available applications to stitch the data, reconstruct the 3D view and quantify (green zone).
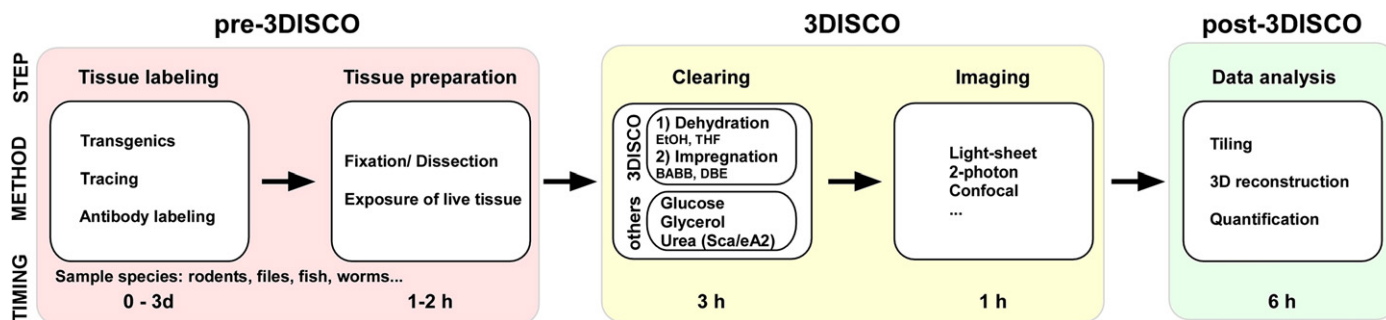
such as the injured spinal cord is processed. After an injury, blood flows out from the vessels and accumulates in the extracellular space. Hence, it is difficult or sometimes impossible to apply 3DISCO on acute pathological tissues (e.g. 2 days post-injury) after big traumatic lesions (Erturk A, unpublished observations) because of the large amount of blood retained in the tissue. Even though most of the blood in the extracellular space is cleared within a few weeks, there might still be residual blood as well as a sturdy scar (Silver and Miller, 2004) hindering clearing and imaging of entire tissue, especially after big traumatic lesions such as a dorsal column hemi-section. Other examples of tissues, which are harder to apply 3DISCO on, include calcified structures such as bones and connective tissue dense structures such as cartilages. Because of their dense assembly, the clearing will require longer incubation times.

Additional limitations come with the currently available imaging technologies that can perform only a limited degree of high-resolution scans on very large tissues. Light-sheet ultramicroscopy is a good option but it is still limited to a resolution of ~2 µm with a 4–5 mm and ~5 µm with 15 mm imaging fields (Dodt et al., 2007; Menzel, 2011). While this resolution would be sufficient to image most of the neuronal cell bodies and some of the dendritic and axonal structures, it will not resolve small structures, including small diameter unmyelinated axons. To overcome this obstacle, we used 2-photon microscopy with high NA objectives (20× with 0.9 NA and 25× with 1.05 NA), which can reach up to 0.5 µm z-resolution and 2.2 mm imaging depth (Figs. 3C and D, Video 4), (Erturk et al., 2012). However, these objectives have a significantly smaller imaging field compared to ultramicroscopy (0.5–0.6 mm vs. 5–15 mm) and, therefore, require multiple z-scans to cover the same size of tissue. In the future, the development of objectives with larger imaging fields and a NA as high as 1–1.5 will greatly facilitate high-resolution imaging of large tissues. Last but not least, difficulty in analysis of large data sets can be listed as a limiting factor. The overwhelming amount of data can make it difficult to focus on key points of the acquired data and to find systematic ways to analyze them. We recently developed algorithms to automate detection and quantification of glia cells and axonal extensions in large 3D image data sets acquired by imaging of cleared adult spinal cord (Erturk et al., 2012). Still, analyzing different morphologies requires dedicated automation tools, and it will take further efforts to develop appropriate automation tools.

To sum up, there are various limitations of the technique, including redefining the method for some specimens that remain difficult to clear, further development of automation tools to handle the large data amounts and to use clearing in living animals. We expect that further developments of 3DISCO will help to overcome these obstacles.

Conclusions

In this review, we have discussed recent advances in 3DISCO along with other popular clearing and imaging methods. 3DISCO achieves high-resolution imaging of large tissues using optical clearing and subsequent imaging by ultramicroscopy or 2-photon, a process which, altogether, can be completed within a few hours (Table 1). Optical clearing decreases scattering of imaging light, hence, provides higher imaging resolution and deeper access into tissue. It is easy and fast to perform on various organisms and tissues. Subsequently, the cleared tissues can be imaged by various imaging techniques. To date, THF and DBE based clearing techniques are the most effective in preserving the fluorescent signal and rendering the tissue transparent. The tissues can be labeled by any method, including endogenous fluorescent expression, tracing with synthetic dyes or staining with antibodies. In addition to naïve tissue, pathological tissues can be cleared. Subsequently, cleared tissues can be imaged using various microscopy techniques, including light-sheet ultramicroscopy, widefield epifluorescence, confocal, 2-photon microscopy, light microscopy and OCT. Therefore, 3DISCO is a unique technique that can offer fast acquisition of high-resolution 3D histological data from the unsectioned organs in heath and disease.

Supplementary data to this article can be found online at http://dx.doi.org/10.1016/j.expneurol.2012.10.018.

References

Becker, K., Jahrling, N., Saghafi, S., Weiler, R., Dodt, H.U., 2012. Chemical clearing and dehydration of GFP expressing mouse brains. PLoS One 7, e33916.

Bijlsma, W.R., Stilma, J.S., 2005. Optical coherence tomography, an important new tool in the investigation of the retina. Ned. Tijdschr. Geneeskd. 149, 1884–1891.

Boas, D., 1997. A fundamental limitation of linearized algorithms for diffuse optical tomography. Opt. Express 1, 404–413.

Briggman, K.L., Denk, W., 2006. Towards neural circuit reconstruction with volume electron microscopy techniques. Curr. Opin. Neurobiol. 16, 562–570.

Bucher, D., Scholz, M., Stetter, M., Obermayer, K., Pfluger, H.J., 2000. Correction methods for three-dimensional reconstructions from confocal images: I. Tissue shrinking and axial scaling. J. Neurosci. Methods 100, 135–143.

Campagnola, P.J., Loew, L.M., 2003. Second-harmonic imaging microscopy for visualizing biomolecular arrays in cells, tissues and organisms. Nat. Biotechnol. 21, 1356–1360.

Cicchi, R., Sampson, D., Massi, D., Pavone, F., 2005. Contrast and depth enhancement in two-photon microscopy of human skin ex vivo by use of optical clearing agents. Opt. Express 13, 2337–2344.

Dent, J.A., Polson, A.G., Klymkowsky, M.W., 1989. A whole-mount immunocytochemical analysis of the expression of the intermediate filament protein vimentin in Xenopus. Development 105, 61–74.

Diaz, R.S., Monreal, J., Regueiro, P., Lucas, M., 1992. Preparation of a protein-free total brain white matter lipid fraction: characterization of liposomes. J. Neurosci. Res. 31, 136–145.

Dodt, H.U., Leischner, U., Schierloh, A., Jahrling, N., Mauch, C.P., Deininger, K., Deussing, J.M., Eder, M., Zieglgansberger, W., Becker, K., 2007. Ultramicroscopy: three-dimensional visualization of neuronal networks in the whole mouse brain. Nat. Methods 4, 331–336.

Erturk, A., Hellal, F., Enes, J., Bradke, F., 2007. Disorganized microtubules underlie the formation of retraction bulbs and the failure of axonal regeneration. J. Neurosci. 27, 9169–9180.

Erturk, A., Mauch, C.P., Hellal, F., Forstner, F., Keck, T., Becker, K., Jahrling, N., Steffens, H., Richter, M., Hubener, M., et al., 2012. Three-dimensional imaging of the unsectioned adult spinal cord to assess axon regeneration and glial responses after injury. Nat. Med. 18, 166–171.

Fuchs, E., Jaffe, J., Long, R., Azam, F., 2002. Thin laser light sheet microscope for microbial oceanography. Opt. Express 10, 145–154.

Fujimoto, J.G., Pitris, C., Boppart, S.A., Brezinski, M.E., 2000. Optical coherence tomography: an emerging technology for biomedical imaging and optical biopsy. Neoplasia 2, 9–25.

Galanzha, E.I., Tuchin, V.V., Solovieva, A.V., Stepanova, T.V., Luo, Q., Cheng, H., 2003. Skin backreflectance and microvascular system functioning at the action of osmotic agents. J. Phys. D: Appl. Phys. 36, 1739.

Genina, E.A., Bashkatov, A.N., Sinichkin, Y.P., Tuchin, V.V., 2006. Optical clearing of the eye sclera in vivo caused by glucose. Quantum Electron. 36, 1119.

Genina, E.A., Bashkatov, A.N., Tuchin, V.V., 2010. Tissue optical immersion clearing. Expert Rev. Med. Devices 7, 825–842.

Gerger, A., Koller, S., Kern, T., Massone, C., Steiger, K., Richtig, E., Kerl, H., Smolle, J., 2005. Diagnostic applicability of in vivo confocal laser scanning microscopy in melanocytic skin tumors. J. Invest. Dermatol. 124, 493–498.

Gonzalez-Bellido, P.T., Wardill, T.J., 2012. Labeling and confocal imaging of neurons in thick invertebrate tissue samples. Cold Spring Harb. Protoc. 2012.

Hama, H., Kurokawa, H., Kawano, H., Ando, R., Shimogori, T., Noda, H., Fukami, K., Sakaue-Sawano, A., Miyawaki, A., 2011. Scale: a chemical approach for fluorescence imaging and reconstruction of transparent mouse brain. Nat. Neurosci. 14, 1481–1488.

Helmstaedter, M., Mitra, P.P., 2012. Computational methods and challenges for large-scale circuit mapping. Curr. Opin. Neurobiol. 22, 162–169.

Huisken, J., Swoger, J., Del Bene, F., Wittbrodt, J., Stelzer, E.H., 2004. Optical sectioning deep inside live embryos by selective plane illumination microscopy. Science 305, 1007–1009.

Jahrling, N., Becker, K., Schonbauer, C., Schnorrer, F., Dodt, H.U., 2010. Three-dimensional reconstruction and segmentation of intact Drosophila by ultramicroscopy. Front. Syst. Neurosci. 4, 1.

Knuttel, A., Bonev, S., Knaak, W., 2004. New method for evaluation of in vivo scattering and refractive index properties obtained with optical coherence tomography. J. Biomed. Opt. 9, 265–273.

Laskowski, C.J., Bradke, F., 2012. In vivo imaging: a dynamic imaging approach to study spinal cord regeneration. Exp. Neurol. http://dx.doi.org/10.1016/j.expneurol.2012.07.007.

Leischner, U., Zieglgansberger, W., Dodt, H.U., 2009. Resolution of ultramicroscopy and field of view analysis. PLoS One 4, e5785.

Menzel, R., 2011. Ultramicroscopy — imaging a whole animal or a whole brain with micron resolution. Front. Neurosci. 5, 11.

Mertz, J., Kim, J., 2010. Scanning light-sheet microscopy in the whole mouse brain with HiLo background rejection. J. Biomed. Opt. 15, 016027.

Muller, D., Jagla, T., Bodart, L.M., Jahrling, N., Dodt, H.U., Jagla, K., Frasch, M., 2010. Regulation and functions of the lms homeobox gene during development of embryonic lateral transverse muscles and direct flight muscles in Drosophila. PLoS One 5, e14323.

Ott, S.R., 2008. Confocal microscopy in large insect brains: zinc-formaldehyde fixation improves synapsin immunostaining and preservation of morphology in whole-mounts. J. Neurosci. Methods 172, 220–230.

Parra, S.G., Chia, T.H., Zinter, J.P., Levene, M.J., 2010. Multiphoton microscopy of cleared mouse organs. J. Biomed. Opt. 15, 036017.

Peng, H., Ruan, Z., Long, F., Simpson, J.H., Myers, E.W., 2010. V3D enables real-time 3D visualization and quantitative analysis of large-scale biological image data sets. Nat. Biotechnol. 28, 348–353.

Plotnikov, S., Juneja, V., Isaacson, A.B., Mohler, W.A., Campagnola, P.J., 2006. Optical clearing for improved contrast in second harmonic generation imaging of skeletal muscle. Biophys. J. 90, 328–339.

Regar, E., Schaar, J.A., Mont, E., Virmani, R., Serruys, P.W., 2003. Optical coherence tomography. Cardiovasc. Radiat. Med. 4, 198–204.

Schonbauer, C., Distler, J., Jahrling, N., Radolf, M., Dodt, H.U., Frasch, M., Schnorrer, F., 2011. Spalt mediates an evolutionarily conserved switch to fibrillar muscle fate in insects. Nature 479, 406–409.

Siedentopf, H., Zsigmondy, R., 1902. Uber Sichtbarmachung und Größenbestimmung ultramikoskopischer Teilchen, mit besonderer Anwendung auf Goldrubingläser. Ann. Phys. 315, 1–39.

Sillitoe, R.V., Hawkes, R., 2002. Whole-mount immunohistochemistry: a high-throughput screen for patterning defects in the mouse cerebellum. J. Histochem. Cytochem. 50, 235–244.

Silver, J., Miller, J.H., 2004. Regeneration beyond the glial scar. Nat. Rev. Neurosci. 5, 146–156.

Silvestri, L., B A, Sacconi, L, Iannello, G., Pavone, F.S., 2012. Confocal light sheet microscopy: micron-scale neuroanatomy of the entire mouse brain. Opt. Express 20, 20582–20598.

Smith, R.M., Black, A.J., Velamakanni, S.S., Akkin, T., Tolkacheva, E.G., 2012. Visualizing the complex 3D geometry of the perfusion border zone in isolated rabbit heart. Appl. Opt. 51, 2713–2721.

Sotelo, C., 2003. Viewing the brain through the master hand of Ramon y Cajal. Nat. Rev. Neurosci. 4, 71–77.

Spalteholz, W., 1914. Über das Durchsichtigmachen von menschlichen und tierischen Präparaten. S. Hierzel, Leipzig.

Starr, D., Hixon, R.M., 1943. Tetrahydrofuran. Org Synth, 2, p. 566.

Tuchin, V., 2007. Tissue Optics: Light Scattering Methods and Instruments for Medical Diagnosis. SPIE Press, Bellingham, WA, USA.

Tuszynski, M.H., Steward, O., 2012. Concepts and methods for the study of axonal regeneration in the CNS. Neuron 74, 777–791.

Tyszka, J.M., Fraser, S.E., Jacobs, R.E., 2005. Magnetic resonance microscopy: recent advances and applications. Curr. Opin. Biotechnol. 16, 93–99.

Vargas, G., Chan, E.K., Barton, J.K., Rylander III, H.G., Welch, A.J., 1999. Use of an agent to reduce scattering in skin. Lasers Surg. Med. 24, 133–141.

Vargas, G., Readinger, A., Dozier, S., Welch, A., 2002. Chemical agents for the reduction of light scattering in tissue: implications for light therapeutic applications. Proc. SPIE 4609.

Voie, A.H., Burns, D.H., Spelman, F.A., 1993. Orthogonal-plane fluorescence optical sectioning: three-dimensional imaging of macroscopic biological specimens. J. Microsc. 170, 229–236.

Wen, X., Mao, Z., Han, Z., Tuchin, V.V., Zhu, D., 2010. In vivo skin optical clearing by glycerol solutions: mechanism. J. Biophotonics 3, 44–52.

Wen, X., Jacques, S.L., Tuchin, V.V., Zhu, D., 2012. Enhanced optical clearing of skin in vivo and optical coherence tomography in-depth imaging. J. Biomed. Opt. 17, 066022.

Yasui, T., Tohno, Y., Araki, T., 2004. Characterization of collagen orientation in human dermis by two-dimensional second-harmonic-generation polarimetry. J. Biomed. Opt. 9, 259–264.

Ylera, B., Erturk, A., Hellal, F., Nadrigny, F., Hurtado, A., Tahirovic, S., Oudega, M., Kirchhoff, F., Bradke, F., 2009. Chronically CNS-injured adult sensory neurons gain regenerative competence upon a lesion of their peripheral axon. Curr. Biol. 19, 930–936.

Yokomizo, T., Yamada-Inagawa, T., Yzaguirre, A.D., Chen, M.J., Speck, N.A., Dzierzak, E., 2012. Whole-mount three-dimensional imaging of internally localized immuno-stained cells within mouse embryos. Nat. Protoc. 7, 421–431.

Zhao, Q.L., Guo, Z.Y., Wei, H.J., Yang, H.Q., Si, J.L., Xie, S.S., Wu, G.Y., Zhong, H.Q., Li, L.Q., Guo, X., 2011. In vivo reflectance spectroscopy study of different clearing agents on human skin optical clearing. Guang Pu Xue Yu Guang Pu Fen Xi 31, 302–307.

Zipfel, W.R., Williams, R.M., Christie, R., Nikitin, A.Y., Hyman, B.T., Webb, W.W., 2003. Live tissue intrinsic emission microscopy using multiphoton-excited native fluorescence and second harmonic generation. Proc. Natl. Acad. Sci. U. S. A. 100, 7075–7080.